

SHAPE MEMORY PROPERTIES OF FeNiCoTi RIBBONS EVIDENCED BY MAGNETIC MEASUREMENTS

F. TOLEA, M. SOFRONIE*, M. TOLEA, V. KUNCSEK, M. VALEANU
National Institute of Materials Physics, 077125 Bucharest, Romania

The present work addresses the shape memory and (ferro)magnetic properties of $\text{Fe}_{52}\text{Ni}_{29-x}\text{Co}_{15+x}\text{Ti}_4$ (with $x=0, 3$ and 6) alloys. The analysed samples were prepared as ribbons by the melt spinning method and subjected to thermal treatments. X-ray diffraction, DSC, thermomagnetic measurements and Mössbauer spectroscopy were used for a complete structural and magnetic characterization. Both the preparation route and the different Co addition induce specific effects which are discussed in detail. The sample with $x=0$ sustains an irreversible transformation, while a partial reversible transformation and a relatively increased Curie temperature were observed for sample with $x=3$. However, further increasing the Co content to $x=6$ leads to a loss of the martensitic transformation.

(Received March 20, 2015; Accepted May 27, 2015)

Keywords: Ferromagnetic Shape Memory Alloys; Martensitic transformation; Magnetic properties; Mössbauer Spectroscopy,

1. Introduction

Specific for Shape Memory Alloys (SMAs) in metallic alloys is the so called martensitic transformation (MT), which is a thermoelastic reversible structural phase transition between high symmetry γ (austenite) and low symmetry α' (martensite) phases. Ferromagnetic Shape Memory Alloys (FSMA) are materials in which MT lies in the temperature region of magnetic order. These alloys give rise to a class of active materials with expected potential to produce both the large actuator strain of shape memory alloys and the rapid response of magnetostrictive materials. Besides the well known Ni_2MnGa [1, 2] Fe-Mn-Si [3, 4, 5] and Fe-Pd [6], the Fe-Ni-Co-Ti based alloys [7] are promising FSMA because of the lower material cost, high productivity, better cold-workability, high ductility and strong magnetization (e.g. with a saturation magnetization nearly three times stonger that of Ni-Mn-Ga [8]).

For FeNiCoTi alloys, the most important prerequisite for the Shape Memory Effect (SME) is the formation in the austenitic phase of fine dispersed and coherent $(\text{Ni,Co,Fe})_3\text{Ti}$ particles which form the so called γ' phase (FCC ordered with $L1_2$ structure). This phase is directly connected with the reversibility of the transformation by ensuring the thermoelastic martensite. Many efforts have been directed towards tuning the martensitic transformation from non-thermoelastic (without involving γ' phase) to thermoelastic [9]. Specific thermal treatments (ausaging) are usual procedures for introducing and controlling conventional SME. The finely dispersed γ' phase particles (coherent with austenite) formed during ausaging, are thought to promote thermoelasticity through the increase of the austenite hardness. We mention here that in the literature there are different opinions regarding the active phase suffering MT. Some researchers argue that the role of γ' is to strengthen the principal γ austenitic phase, suppressing plastic-flow processes during $\gamma \leftrightarrow \alpha'$ MTs. However, the γ' disperse grains do not undergo MTs,

*Corresponding author: mihsosof@infim.ro

but they favour the accumulation of the elastic energy in martensite crystals through the modification of the degree of tetragonality [10, 11]. The large tetragonality of the BCT α' martensite could induce fine twinning structure in martensite phase due to the low twinning boundary energy [12]. Thus, Maki et al. [9] reported $\gamma \rightarrow \alpha'$ (face-centered cubic, FCC, to body-centered tetragonal, BCT) thermoelastic martensitic transformation, which is a result of the precipitation of γ' -Ni₃Ti (L1₂), in a FeNiCoTi alloy. Another opinion (Kubla and E. Hornbogen [13]) is that γ' precipitates initially generated in austenite transform into martensite without losing their coherency and thus, these particles become α' . As we will show in the following, the results presented in this paper in line with our previous results [14] support rather the second opinion.

The so formed γ' particles have to be small enough to be active along the MT. During the MT, they are sheared in a metastable structure and store, thereby, elastic back-stress. In such condition the transformation leads to an elastic deformation of the austenitic matrix. Concerning the optimal size of the γ' particles, [11, 13, 15, 16] these are imposed by the coherence condition, e.g. they are coherent with austenite for average diameters of less than 10 nm and begin to lose rapidly their coherence for larger sizes. Coherent γ' nanoparticles favour the formation of thin plate like, thermoelastic martensite under cooling. For increased aging time, the size of γ' nanoparticles start to grow and the incoherent zones become larger, with the further formation of transformation products of lenticular or butterfly martensites, which do not keep the thermoelasticity. The main element in the γ' precipitates of type (Fe,Ni,Co)₃Ti is Ni (with more than 50%, according to R.Hayashi [7]), but each particular composition depends on the initial Co content in the alloy. In fact, the Co substitution on the Ni sites has a significant role on both the shape memory effects and related parameters (e.g. the magnitude of the effect and the saturation magnetization, M_S) as well as on the magnetic behaviour (e.g. magnetic anisotropy and the Curie temperature). By tuning the Co content, it becomes possible to tune the martensitic transformation temperatures as well as the magnetic transition temperatures, with respect to the room temperature (RT), with a large impact on various applications of such FSME systems. A critical issue of the alloy is large thermal hysteresis, with an austenite finish temperature, A_f (during heating for reaching austenite from martensite) well above RT. However this heating process leads the sample in the temperature range at which diffusion becomes active and a new undesired η phase is formed. The precipitation of incoherent and stable η phase (DO₂₄ hexagonal Ni₃Ti) leads to a deterioration of the shape recovery [14, 17, 18, 19].

We emphasize in the following that for SMAs, the structure and the mobility of the boundaries between austenite and martensite are very important with respect to a suitable thermoelastic transformation of narrow temperature hysteresis. The austenite/martensite phase boundaries (interface of transformation) should not be blocked by dislocations, which might lead to the formation of more irreversible martensite [20].

In the present work, we propose a careful consideration of the effects induced on the structural and magnetic properties of Fe-Ni-Co-Ti alloys by different substitutions with Co atoms on the Ni sites. The results obtained from X-ray diffraction (XRD), differential scanning calorimetry (DSC), magnetometry and Mössbauer spectroscopy (MS) are discussed in regard to the phase transformation processes reported in the literature. Compositions with narrow thermal hysteresis and convenient MT temperatures were obtained. Starting from the well known idea that in FSMA the MT temperatures decrease with decreasing concentration of valence electrons per formula unit (e/a) [21], we have considered those compositions in which a part of Ni atoms are substituted by Co atoms. Besides the decrease of the electronic concentration and so of the TM temperature, an increase of both the saturation magnetization and Curie temperature was also intended by this substitution.

2. Experimental

Intermetallic compositions of Fe₅₂Ni_{29-x}Co_{15+x}Ti₄, with x= 0, 3 and 6 were prepared from metallic elements by arc melting in argon atmosphere. The as obtained samples were subsequently rapidly quenched by the melt spinning technique, resulting ribbons of about 30 μ m thicknesses, 3

mm wide and 30 to 70 mm long. A thermal treatment devoted to sample homogenization as well to the segregation of the γ' phase was performed on some rapidly quenched ribbons in vacuum, for 5 min at 950K. These annealed samples are denoted as P1 for $\text{Fe}_{52}\text{Ni}_{29}\text{Co}_{15}\text{Ti}_4$ ($x=0$), P2 for $\text{Fe}_{52}\text{Ni}_{26}\text{Co}_{18}\text{Ti}_4$ ($x=3$) and P3 for $\text{Fe}_{52}\text{Ni}_{23}\text{Co}_{21}\text{Ti}_4$ ($x=6$).

The temperature induced structural transformations were evidenced by temperature dependent energy-dispersive x-ray diffraction (EDXRD) using synchrotron radiation at HASY-LAB, F2.1 beam line/DESY, Hamburg, Germany. In order to characterize the martensitic transformation (transformation temperatures and thermal hysteresis) we performed DSC scans with a scanning rate of 20 K/min, by a 204 F1 Phoenix NETZSCH device. Magnetic measurements were performed at high temperatures on a PPMS (Quantum Design) working under Vibrating Sample Magnetometry (VSM) option. The low temperature magnetic measurements were performed with a High Field measurement system (Cryogenic Ltd.) working also in the VSM mode.

Mössbauer Spectroscopy measurements between 80 K and 295 K have been performed by inserting the samples in a static Helium/Nitrogen bath cryostat. A ^{57}Co source in Rhodium matrix and a spectrometer working in constant acceleration mode in transmission geometry were used. The calibration was made by using α -Fe metallic foil at RT and the isomer shifts were reported accordingly.

3. Results and discussions

We start by presenting the XRD patterns versus temperature, as obtained with synchrotron radiation at HASYLAB- DESY by cooling sample P1 from 300 K down to 50K (Fig.1a). As shall be discussed, the results show a martensitic transformation in a very wide temperature range. The diffraction peaks at room temperature (Fig.1a, upper curve) correspond to a typical face-centered cubic (fcc) structure for P1 sample. However, they are relatively broad due to the dispersion of crystallite sizes - as specific for the preparation route - and one cannot exclude the presence of an additional phase of similar structure (e.g. the γ' phase). Such γ' particles with CuAu-like fcc structure and lattice parameters almost the same as for the γ matrix have been reported previously [15]. By lowering the temperature, at about 200 K (below the martensite start temperature, M_s), the phase transition is initiated and the body-centered tetragonal (bct) martensitic phase appears in addition to the remaining cubic γ - fcc phase. The γ structure is still present in a small amount even at 50 K (below martensite finish temperature M_f), meaning that not the entire austenitic phase supports the MT. In accordance with [13, 14], also γ' is expected to be transformed into α' - bct martensitic phase, only a part of the γ phase remaining untransformed. In addition, according to the same Fig 1a, after the first cooling at 50K, when reversing at 300 K - see the lowest curve - the specific structure of martensitic phase is still present. This irreversibility is indicated also by VSM thermo-magnetic scans as well as by Mössbauer spectroscopy – as shall be discussed later in this section. However, no MT is observed by temperature dependent XRD in sample P3 in the temperature interval 300 K to 17 K. This sample presents peaks corresponding to both body-centered cubic (bcc) and γ (fcc) phases (Fig.1b), almost unchanged over the whole temperature interval. Similar conclusions were also obtained by typical calorimetric measurements (not shown here) performed by a differential scanning calorimeter (DSC- 204 F1 Phoenix, Netzsch) with a scanning rate of 20K/min. However, due to the very wide thermal hysteresis, the enthalpies are difficult to be detected in such measurements.

The low temperature magnetic measurements obtained in the VSM mode for all three samples are shown in Fig.2a. Contrary to P1 and P2 samples which open thermal hysteresis, the measurements performed on sample P3 reveal no structural transformation of first order. These results are consistent with temperature dependent Mössbauer spectroscopy (Fig.3 P3) and XRD measurements (Fig1b). As seen from Fig.2a, the magnetic measurements allow a relatively accurate detection of the martensite start temperatures, which are 240K and 190K for samples P1 and P2, respectively.

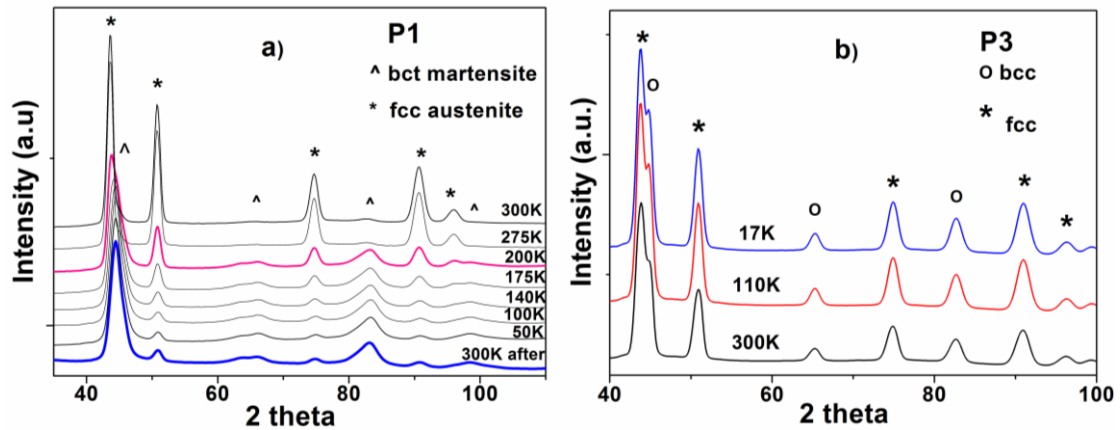


Fig.1a) Temperature dependent XRD patterns of sample P1 by cooling from 300 K down to 50 K and back at 300K ; b) XRD patterns of P3 sample collected at decreasing temperatures down to 17 K.

If after the first cooling - heating cycle from 290 K down to 70 K and then back to room temperature, P2 sample is cooled again at 70 K, it is to be noted that the magnetization vs. temperature follows the same path (see inset of Fig. 2a). Hence, there is direct evidence that P2 sample does not undergo a second time the martensitic transformation because it does not reach not only the required austenite finish temperature (A_f), but even the austenite start temperature (A_s). One can argue that the magnetization is larger at low temperatures after this second cooling, due to the residual martensite which remains in the austenite matrix after the first cooling.

It can be seen that the difference in magnetization at 290 K, after a heating-cooling cycle, is smaller for P2 sample than for P1, suggesting a less active phase in P2. This aspect may probably be improved by a longer/optimal heat treatment aimed to an increased amount of the γ' active phase.

The experimental results showing the magnetization as a function of temperature (sample P1) as obtained on the PPMS device are presented in Fig.2b. Two different magnetic phases are evidenced: the first magnetic phase has the Curie temperature of approx. 550K and can be attributed to the γ phase not involved in the austenite-martensite transition. The second magnetic phase, with T_c approx. 1000 K can be assigned to the fine dispersed $(FeNiCo)_3Ti$ phase (γ') directly connected with the reversibility of the transformation, because it favours the occurrence of tetragonal martensite. As we shown in [14], this second phase could become unstable (if the sample is heated for a too long time or at a too high temperature) and transforms into incoherent precipitates (η phase) which deteriorates the shape recovery. A new thermo-magnetic VSM measurement has started on a new P1 sample from 300 K (see inset of Fig 2b), by following the sequence: cooling down the sample to 150K (curve 1), heating it up to 650K (curve 2) and cooling it back to 300 K (curve 3). The shift in magnetization at RT between the two measurements can be explained by an incomplete transformation of the high temperature austenite phase into martensite, putting in evidence the irreversibility or partial reversibility of the MT in sample P1. This may be due to exceeding the critical size of γ' phase [10], to loss of coherence with austenitic matrix/appearance of lenticular martensite, or even to the formation of more thermodynamically stable η phase, incoherent with the mother matrix [14, 22].

Concerning the measurements in low, respectively high magnetic fields (see Fig. 2b), it can be seen the sharp decrease of magnetization during the cooling process in 200 Oe (curve 1 in Fig.2b) correlated with the increase of magnetization after cooling in 5 T (curve 1-inset of Fig.2b) after reaching martensite start temperature M_{st} . It is associated with the increase of the magneto-crystalline anisotropy induced by the structural transformation from cubic fcc austenite to bct martensite. This behaviour certainly proves a change in magneto-crystalline anisotropy during the MT. At low fields, due to its smaller magneto-crystalline anisotropy, the austenite phase is easier magnetized than the martensite, giving rise to a higher magnetization. By cooling the sample and

passing through the M_{st} temperature, magnetization shows a reduction (due to the lower magnetization of the martensite state with higher anisotropy); the low magnetic field does not succeed to rotate the magnetic moments in the field direction, or to produce enough driving force to move the twin boundary of the variant whose easy axis is aligned with the field. Therefore, the measured martensite magnetization is small. For high enough fields, by passing from austenite to martensite, at M_s , the magnetization shows an augmentation, demonstrating that martensite phase has a higher magnetization at saturation. The same behaviour was evidenced on Ni_2MnGa single crystal [8, 23] and $Ni-Fe-Ga$ alloy [24, 25] with a direct influence on the hysteresis area. The interpretation of this behaviour can be emphasized by taking into account the magnetization curves assigned to a pure austenite phase with low anisotropy and to a pure martensite phase with high anisotropy, respectively [24].

A very large hysteresis (located in the temperature region where the two phases coexist) is suggested between the cooling and heating curves of VSM measurements (Fig. 2a and Fig.2b). This thermo-magnetic scan validates the fact that the thermal hysteresis is a characteristic of a first order phase transition. This is consistent with the literature being a strong indication that $FeNiCoTi$ materials exhibit large magnetic anisotropy energy (the difference in magnetization-applied field behaviour between easy and hard axis) to facilitate martensite variant motion under applied fields [26, 27].

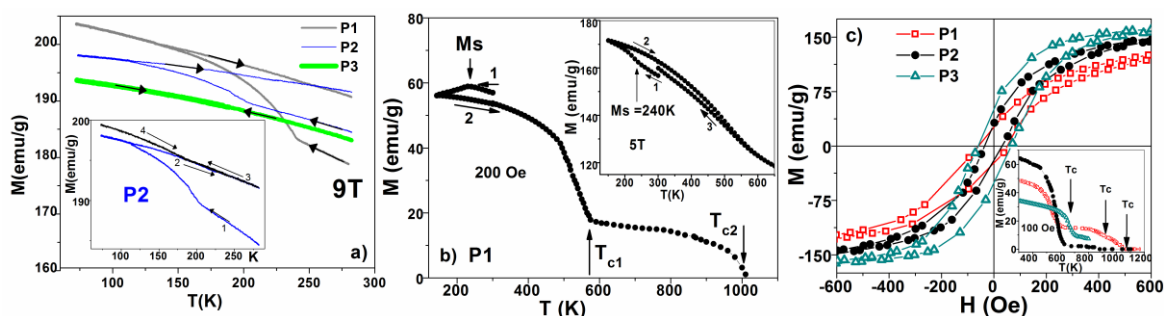


Fig.2. a): Low temperature thermo-magnetic measurements performed in the VSM mode under an applied field of 9T. Inset: P2 sample cooled-heated a second time at room temperature downward. b) VSM thermo-magnetic scans performed in low magnetic field (200 Oe) for P1 sample evidence two different magnetic phases. The martensite start temperature is $M_{st} = 240$ K. Inset: thermo-magnetic measurements performed in high field (5T) for P1 in a new cooling-heating cycle; c) Hysteresis loops collected at RT on the three samples as presented in a narrow field range. Inset: Thermo-magnetic measurements performed for P1, P2 and P3 samples in 100 Oe

The hysteresis curves (Fig.2c) at RT shows that the saturation magnetization is increasing with the Co content and the coercive field of sample P2 is lower than of sample P1. Thermo-magnetic measurements highlight that the Curie temperature (T_c) increases with increasing of Co addition for both γ and γ' phases (Fig.2c Inset). One can notice three stages in the magnetization evolution for the sample P1. The first change corresponds to the T_c of the γ phase, the second can be attributed to the T_c of γ' , while the third may indicate the appearance of a new phase (η) in the sample P1 after heating above 1000 K, with its own T_c . It can be seen here too that there is less active phase in P2 than in P1, as resulting from lower magnetization decay in the second stage (see Inset of Fig.2.a).

Mössbauer spectroscopy measurements have been performed in order to observe structural transformations related to temperature induced variations in local atomic configurations. Mössbauer spectra collected at different temperatures or after different thermal treatments applied to samples P1, P2 and P3 are shown in Fig. 3. The changes in the local configurations can be followed via the evolution of the hyperfine field distributions, shown on the right hand of the spectra. Through its high sensitivity to the local structure around Fe atoms, Mössbauer spectroscopy succeeded to evidence the martensite – austenite transformation, via the temperature

dependence of the most probable hyperfine field at the Fe nucleus as it is detailed also via Fig.4 a) and b), for samples P1 and P2, respectively. However, as is shown in Fig.3 P3, almost no changes are observed in the RT Mössbauer spectra of sample P3 (as well as in the corresponding magnetic hyperfine field distributions presented on the left side of each spectrum), after different stages of cooling/heating procedures. Hence, both the thermomagnetic measurements and the Mössbauer data have evidenced that an irreversible MT takes place in sample P1, while P2 undergoes a partial reversible transformation and P3 does not support the MT at all.

The probability distribution of the hyperfine field evaluated from the RT Mössbauer spectrum of sample P1 (a large distribution of iron configurations is suggested), is characterized by an average field of 24.4 T and a most probable hyperfine field of 28 T (see first distribution in Fig.3 P1). Taking into account the average value of the isomer shift (IS) reported to metallic iron of about -0.12 mm/s, it can be concluded that the majority phase is an fcc austenitic phase. A less pronounced peak in the distribution probability, located at about 34 T, suggests also the presence of a minority martensitic phase already at this temperature. Successive Mössbauer spectra obtained from 80 K up to RT have evidenced strongly shifted distributions with most probable hyperfine fields of 35 T to 34 T, depending on temperature (see Figs.3 P1 and 4a) which clearly sustains a structural transformation. The values of the average hyperfine field (33.1 T), coupled with an isomer shift of just 0.05 mm/s, support the presence of a bct martensitic phase. In addition, the irreversibility of the transformation is supported by the presence of just the martensite phase at RT after cooling P1 at 80 K. Even the subsequent heating at 400 C for 3 min did not introduce a remarkable reversal of the martensitic phase to austenite. It is worth to mention that after collecting a first Mössbauer spectrum, sample P1 was heated at 400 C for 3 minutes in order to reach A_f temperature for a complete transformation (the large thermal hysteresis may suggest gradual transformation). Since the ribbons were initially annealed at 680C for 5 min, the mentioned procedure would only initialize a new cooling-heating cycle. However, the appearance of the shoulder at hyperfine fields lower than 30 T in the probability distribution (Fig. 3P1-d) indicates that such treatment might initialize a reversible transformation with the austenite start temperature $A_s < 400$ C.

The situation is different for the sample P2, as evidenced by the spectra presented in Fig.3 P2. In its initial state at room temperature, the probability distribution which is much narrower than in P1, has a maximum at 29 T (average hyperfine field of 27.6 T). Together with an average isomer shift of about -0.1 mm/s, the involved hyperfine parameters suggest again the presence of an austenitic phase (slightly different than in P1). After cooling P2 down to 80 K, the hyperfine field distribution is shifting again consistently to higher values (average hyperfine field of 33.0 T and most probable hyperfine field of 34 T). The specific average IS of about 0.05 mm/s, gives evidence for the martensitic transformation at this temperature. By returning back to room temperature, the probability distribution of the hyperfine field (see Fig.3P2 and Fig. 4b) suggests a mixture of martensite and austenite. After the thermal treatment at 400C for 3 min, the two phases are clearly separated (as evidence by the bi-lobar shape of the hyperfine field distribution in Fig 3P2 - d), the austenite content being much higher than in P1 but still lower than the martensite content. Therefore, the Mössbauer data show an almost irreversible transformation for sample P1 and a partially reversible transformation for the sample P2 (with reference to the temperature range 80-300 K).

On the other hand, the P3 sample is different from the previous two. All the probability distributions of hyperfine field evaluated from the Mössbauer spectra in Fig.3 P3 are characterized by the presence of two local maxima, one at about 29 T (attributed to austenitic phase) and another at about 35 T, attributed martensitic phase. In short, almost a same mixture of phases is evidenced in all spectra, independent on the temperature or the applied treatment. By corroborating these data with the results of XRD and thermo-magnetic measurements, we can say that the characteristic structure of this sample is not favourable to martensitic transformation.

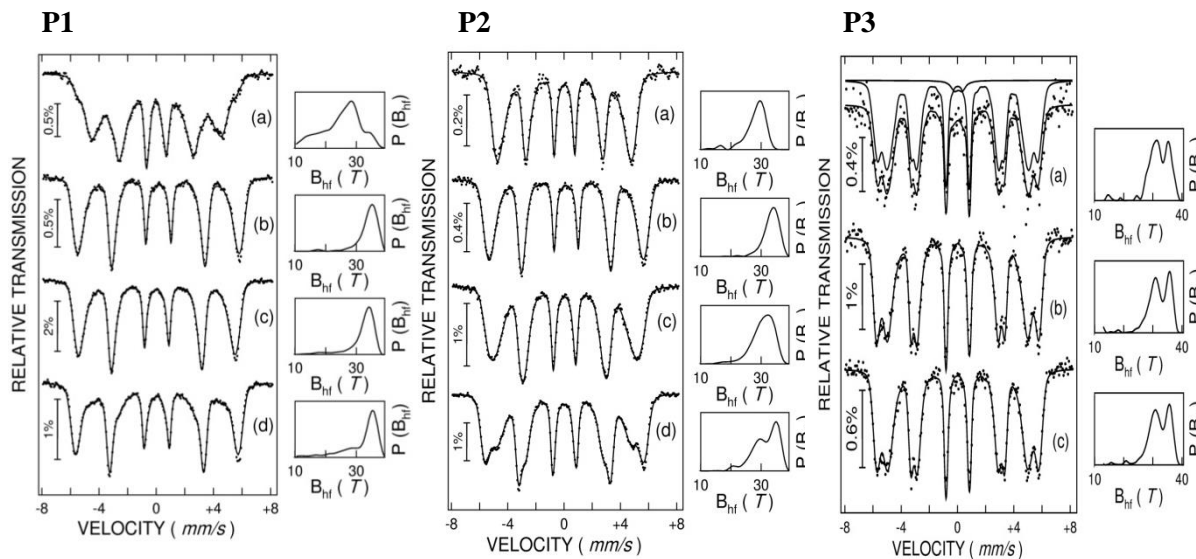


Fig.3: Mössbauer spectra obtained on samples P1, P2, P3, as follows: (a) initial state at 295 K, (b) at a temperature of 80 K, (c) at 295 K, after cooling to liquid nitrogen, (d) at 295 K after heating at 400 K for 3 min. On the right hand are hyperfine field distributions corresponding to each spectrum.

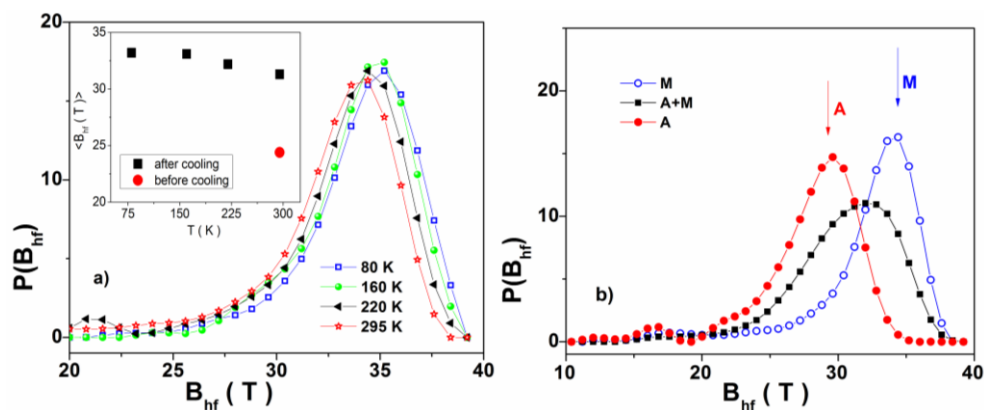


Fig.4 a): The temperature dependent evolution of the probability distribution of hyperfine fields, corresponding to the martensitic phase. In inset is shown the temperature dependence of the average hyperfine field. A consistent difference between the average hyperfine fields of the austenite (before cooling) and martensite (after cooling) phases is observed at the same temperature (RT); b): Probability distributions of hyperfine field for sample P2 in different states: (i) initial state-full circle with mainly austenite phase, (ii) after cooling to nitrogen-open circle with mainly martensite phase and (iii) after returning to room temperature from nitrogen temperature -full square with a mixture of martensite and austenite phases.

4. Conclusions

We have studied the martensitic transformation and magnetic properties of ferromagnetic shape memory alloys $\text{Fe}_{52}\text{Ni}_{29-x}\text{Co}_{15+x}\text{Ti}_4$ (with $x=0, 3$ and 6 referred as P1, P2 and P3 respectively), obtained via an unconventional preparation route consisting of melt spinning and subsequent thermal annealing.

X-ray diffraction and magnetic measurements indicate very wide temperature intervals for the phase transitions and also a wide thermal hysteresis, e.g. the martensite start is at about 240 K for P1 and 190 K for P2, while the austenite finish temperatures are both above 400 K. The sample

P3 did not show a martensitic transformation below room temperature. Large thermal hysteresis may in principle damage reversibility by allowing atomic inter-diffusion and appearance of a ferromagnetic η phase (which does not undergo martensitic transformation), as suggested by measurements of the Curie temperatures. The decrease of martensite start temperature with increasing Co concentration can be associated with decreasing the valence electron concentration per formula unit. Also, increasing the Co content induces an increase in the Curie temperature and saturation magnetization. Thermo-magnetic measurements highlighted that the Curie temperature increases with increasing of Co addition for both γ and γ' fcc phases. Although the Co addition improves the magnetic properties, it also depletes the samples of Ni, impeding the formation of the active γ' phase which is of type $(\text{Fe,Ni,Co})_3\text{Ti}$. The most suitable (in respect to the martensitic transformation) sample P2, contains still too less active phase, an aspect which may be improved by a longer duration of the thermal treatment.

Acknowledgements

This work has been carried out with the financial support of the Romanian Ministry of Education (PN-II-ID-PCE-2012-4-0516 and Core Program 45N). The authors thank to Dr. Balam Sahoo for performing the temperature dependent EDXRD measurements at HASYLAB-DESY in Hamburg, Germany.

References

- [1] J. Gutiérrez, J.M. Barandiarán, P. Lázpita, C. Seguí, E. Cesari, *Sensors and Actuators A: Physical* **129**, 163 (2006);
- [2] D.C. Dunand, P. Müllner, *Advanced Materials*, **23**, 216,(2011);
- [3] K.K. Mahesh, F. M. Braz Fernandes, G. Gurau, *J. of Mat. Sci.* **47**, 6005, (2012);
- [4] M. Valeanu, G. Filoti, V. Kuncser, F. Tolea, B. Popescu, A. Galatanu, G. Schinteie, A.D. Jianu, I. Mitelea, D. Schinle, C.M. Craciunescu, *J. of Mag and Mag. Mat.* **320**, e164,(2008);
- [5] L.G. Bujoreanu, V. Dia, S. Stanciu, M. Susan, and C. Baci, *Eur. Phys. J. Special Topics* **158**, EDP Sciences, Springer-Verlag, (2008);
- [6] M.Sofronie, F. Tolea, V. Kuncser, M. Valeanu, G. Filoti, *IEEE Transactions On Magnetism*, **51**, 2500404 (2015);
- [7] R. Hayashi, S. J. Murray, M. Marioni, S. M. Allen, R. C. O'Handley, *Sensors and Actuators* **81**, 219 (2000);
- [8] S. Murray, R. Hayashi, M. Marioni, S.M. Allen, R.C. O'Handley, *SPIE Conference on Smart Materials Technologies*, Newport Beach California, **3675**, 0277-736X/99 (1999);
- [9] Y. Geng, M. Jin, W. Ren, W. Zhang, X. Jin, *J. All. Comp* **577S**, S631, (2013);
- [10] T. Maki, K. Kobayashi, M. Minato, I. Tamura, *Scripta Metall.* **18**, 1177 (1984);
- [11] Yu.I. Chumlyakov, I.V. Kireeva, E. Yu. Panchenko, E.G. Zakharova, V.A. Kirillov, S.P. Efimenko, and H. Sehitoglu, *Doklady Physics*, **49**, 47 (2004);
- [12] Y. Geng, D. Lee, X. Xu, M. Nagasako, M. Jin, X. Jin, T. Omori, R. Kainuma, *Journal of Alloys and Compounds* **628**, 287, (2015);
- [13] G. Kubla and E. Hornbogen, *Journal de Physique IV*, C8, **5**, 475, (1995);
- [14] F. Tolea, G. Schinteie, B. Popescu, *JOAM* **8**, No.4, 1502, (2006);
- [15] C. Lishan, Y. Dazhi, L. Guobin, Z. Min, *Acta Metallurgica Sinca Series A*, **4**(6), 431 (1991);
- [16] T. Omori et al, *Scripta Mat.* **69**, 812, (2013);
- [17] E. Patoor, D.C. Lagoudas, P.B. Entchev, L. Catherine Brinson, X. Gao, *Mechanics of Materials* **38**, 391, (2006);
- [18] D. Lee, T. Omori, R. Kainuma, *J. All. Comp.* **617**, 120, (2014);
- [19] Yoon-Uk Heo, M. Takeguchi, K. Furuya, Hu-Chul Lee, *Acta Materialia* **57**, 1176, (2009);

- [20] N. Jost, Mat. Sci.and Eng. A, **649**, 273, (1999);
- [21] C. Seguí, J. Pons, E. Cesari, Acta Materialia **55**, 1649, (2007);
- [22] L.G.Bujoreanu, "Materiale Inteligente", Editura Junimea, IASI, (2002);
- [23] J. Pons, E. Cesari, C. Seguí, F. Masdeu, R. Santamarta, Mat. Sci.and Eng. A **481-482**, 57(2007).
- [24] M. Sofronie, F.Tolea, V.Kuncser, M.Valeanu, J. Appl. Phys. **107**, 113905, (2010);
- [25] F. Tolea, M. Sofronie, C. Ghica, M. Valeanu. Opt. Adv. Matt-Rapid Comm., **5**, 562, (2011);
- [26] H. Sehitoglu, C. Efstathiou, H.J. Maier, Y. Chumlyakov, J. of Mag. And Mag. Mat. **292**, 89, (2005);
- [27] T. Kakeshita, K. Shimizu, T. Maki, I. Tamura, S. Kijima, M. Date, Scripta Metall. **19**, 973, (1985);
- [28] S. Kajiwara, Mat.Sci. Eng. A **273-275**, 67, (1999).